Dynamics of two-dimensional frustrated Josephson arrays

Italo F. Marino and Thomas C. Halsey
The James Franck Institute and the Department of Physics, The University of Chicago, Chicago, Illinois 60637
(Received 23 March 1994)

We study two-dimensional frustrated arrays of Josephson junctions at nonzero voltage. There exists a family of traveling-wave solutions characterized by a constant spatial phase shift. All spatially periodic vortex configurations observed in numerical simulations are of this form, and can be parametrized in terms of this single phase shift. We present the analytical form of these solutions at high voltages (or high Josephson frequencies) and compute their I-V characteristics. We also report the numerical observation of relaxational fronts separating two regions with different phase shift and frequency. These fronts move in the direction of decreasing frequency (or voltage).

I. INTRODUCTION

Two-dimensional arrays of Josephson junctions provide a rich laboratory in which to study the dynamics of spatially extended systems.[1] In addition to their theoretical interest, these arrays can be studied experimentally, and have potential applications as coherent oscillators.

One example of the rich dynamics of these arrays is presented by "giant Shapiro steps."[2] These voltage steps correspond to a coherent phase locking of the Josephson oscillations of the individual junctions of the array with an applied rf field. These steps have been extensively studied by experimental, numerical, and analytical techniques.[3]

We here study an intrinsically simpler, but less understood, problem: the state of arrays subjected to dc but not ac currents.[4] We consider frustrated arrays, with transverse applied magnetic fields. We find that, in the limit where the voltage across the junctions is large, the problem simplifies considerably, because the dominant oscillation of the superconducting phases is at the Josephson frequency corresponding to this voltage, with higher harmonics of this frequency suppressed. Thus a single amplitude and two phases (for the dc and the ac components of the superconducting phase difference) define uniquely the state of each junction.

This relatively simple problem allows for an immediate ansatz solution, in terms of one global phase δ, whose value uniquely specifies the state of the array. The overall current flowing across the array is a function of δ, so that there is a band in the I-V plot corresponding to this family of states. The width of this band (in voltage) is inversely proportional to the current at high current. This approach can be easily generalized to lower voltages, although computations become intractable as one approaches the critical current, at which the voltage goes to zero.

We compare our results to numerical simulations of arrays with frustration parameters $f=\frac{1}{2}, \frac{1}{3}$, and $\frac{2}{5}$. This parameter measures the ratio of the magnetic flux linked by one plaquette of the array with the superconducting magnetic flux quantum. A large class of observed states of the array can be indexed by the parameter δ, as hypothesized. However, an additional phenomenon appears, in the form of fronts separating regions of different δ. These fronts move in from the boundary, moving always towards regions of lower voltage. They represent the method by which systems relax their overall values of δ. We believe that the quantitative structure of these fronts is the primary problem left unresolved by this study; in this work we thus do not address the problem of the selection of a particular value of δ by the system.

In Sec. II we review the standard resistively shunted junction (RSJ) model for overdamped Josephson junctions. We then introduce a simplified high-voltage form of the equations of motion for this system. In Sec. III, we present a family of traveling-wave solutions of these equations, which have a combined spatiotemporal symmetry. This is the most spatially homogeneous solution of these equations. In Sec. IV, we generalize these results to moderate voltages, and in Sec. V, we present numerical results. In particular, in this final section we discuss the appearance of moving fronts separating regions of different δ and voltage. We hypothesize that these fronts represent a principal means by which an array relaxes its voltage.

II. THE MODEL AND ITS HIGH-VOLTAGE LIMIT

We consider a square array of overdamped resistively shunted Josephson junctions in a transverse magnetic field, with the flux per unit plaquette being f (in units of the superconducting magnetic flux quantum). If the shunt resistance is R, and the critical current of the junctions is i_0, then the current from the ith to the jth (neighboring) site of the array is

$$I_{ij}=\frac{\hbar}{2eR}\frac{d}{dt}(\theta_i-\theta_j)+i_0\sin(\theta_i-\theta_j-A_{ij})\ , \tag{1}$$

where θ_i is the superconducting phase on the ith site, and $\sum_P A_{ij}=2\pi f$, where the sum is about a plaquette. The first term on the right-hand side of Eq. (1) is the normal shunt current, while the second is the supercurrent. In the overdamped limit, the sum of currents arriving at

each site of the array must equal zero.

Now let us consider such an array driven by a dc current parallel to one of the axes (say, the horizontal axis) of the square lattice. We expect that, on average, the voltage drop across junctions parallel to the direction of current flow will be $v=V/N$, where V is the total average across an $N\times N$ square array. Similarly, we expect zero average voltage across junctions perpendicular to the direction of current flow. Of course, these are assumptions—we cannot exclude the possibility that inhomogeneous average voltage differences may develop in the network.

A further simplification appears if we consider high voltages $v \gg i_0 R$. In this limit, the normal current dominates the supercurrent; effects of the latter are reduced by factors of order $i_0 R/v$. We define a dimensionless group $\kappa \equiv i_0 R/v$; this is the fundamental small parameter of our approach.

The ac Josephson relation implies that a voltage of magnitude v is accompanied by oscillations of the phases $\{\theta_i\}$ of frequency $\omega_J = 2ev/\hbar$.[5] These oscillations will lead in turn to supercurrents, which may include dc components, but will also certainly include ac components at the frequency ω_J and all of its harmonics. We shall see below that, at high voltages, the higher harmonics are suppressed in amplitude by factors of order κ. Thus we shall commence by writing

$$\theta_{mn} = \alpha_{0,mn} + \alpha_{1,mn}\cos(\omega_J t + \phi_{mn}) + n\omega_J t \ , \tag{2}$$

for the site in the mth row and the nth column. The last term on the right-hand side ensures that the average voltage increases by v as one moves one column to the right. Note that typically we will index sites by a single index, such as i. The appearance of two indices mn in Eq. (2) allows us to indicate separately the row and the column of a particular site. It is also convenient to define a directed phase difference $\tilde{\alpha}_{0,ij} \equiv \pm|\alpha_{0,i} - \alpha_{0,j} - A_{ij}|$; the sign of this phase difference is determined by always subtracting the phase to the left from that to the right, on a horizontal bond, or by subtracting the upper phase from the lower phase, on a vertical bond.

For the three undetermined parameters α_0, α_1, and ϕ, we may write three equations at each site of the array. Two of these arise from the cosine and sine components of the currents at frequency ω_J. Since we expect $\alpha_{1,mn} \sim \kappa$, in these equations we may neglect the effect of the oscillating part of θ_{mn} inside the supercurrent term. Simple algebra then yields the following equations:

$$\sum_j \{\alpha_{1,i}\cos(\phi_i) - \alpha_{1,j}\cos(\phi_j) - \kappa\cos(\tilde{\alpha}_{0,ij})\} = 0 \ , \tag{3}$$

$$\sum_j \{\alpha_{1,i}\sin(\phi_i) - \alpha_{1,j}\sin(\phi_j) - \kappa\sin(\tilde{\alpha}_{0,ij})\} = 0 \ , \tag{4}$$

where the sum is over sites adjacent to site i. Note that $\alpha_1 \sim \kappa$, which is consistent with our assumptions. Let us write

$$\alpha_{1,i}\cos(\omega_J t + \phi_i) - \alpha_{1,j}\cos(\omega_J t + \phi_j) \equiv \tilde{\alpha}_{ij}\cos(\omega_J t + \tilde{\phi}_{ij}) \ , \tag{5}$$

thereby defining an effective amplitude and phase shift for the oscillating part of the phase difference across the $\langle ij \rangle$ bond. We then can combine Eqs. (3) and (4):

$$\sum_j \left\{\exp(i\tilde{\alpha}_{0,ij}) - \frac{\tilde{\alpha}_{ij}}{\kappa}\exp(i\tilde{\phi}_{ij})\right\} = 0 \ . \tag{6}$$

Turning now to the dc part of the current, we see that the supercurrent flowing along the vertical bonds must balance the average supercurrent flowing along the horizontal bonds. The latter appears because of the influence of the oscillating phase difference inside the supercurrent term, as in the analogous theory of supercurrent flow with rf voltage driving.[6] We can easily obtain

$$\sum_{j_\perp} \sin(\alpha_{0,i} - \alpha_{0,j} - A_{ij}) + \sum_{j_\parallel} J_1(\pm\tilde{\alpha}_{ij})\cos(\alpha_{0,i} - \alpha_{0,j} - A_{ij} - \tilde{\phi}_{ij}) = 0 \ , \tag{7}$$

where J_1 is the Bessel function, and $j_\parallel, j_\perp$ indicate respectively the neighbors in the horizontal and vertical directions (respectively, the directions parallel and perpendicular to the mean current flow). The minus sign of the Bessel function argument is taken for the bond to the left, and the plus sign is taken for the bond to the right.

III. THE TRAVELING-WAVE STATES

Now we turn to possible solutions of these equations. It is clear from Eq. (7) that the gauge-invariant phase difference $\alpha_{0,i} - \alpha_{0,j} - A_{ij} \sim \kappa$ on vertical bonds. In fact, in our numerical studies this quantity was exactly zero in the observed spatially periodic solutions. If it were not zero, then an average supercurrent would flow locally perpendicular to the direction of mean current flow, which would clearly break the translational symmetry of the array. This numerical result thus suggests that we may profitably restrict ourselves to the study of solutions with combined translational and time-translational symmetry. In practice, this means (as will be seen below) that translation of the solution by a time $\tau = 2\pi f/\omega_J$ is equivalent to a spatial translation by one lattice spacing in the vertical direction (perpendicular to the mean current flow), and a translation by the time $\tau = \delta/\omega_J$ is equivalent to a spatial translation by one lattice spacing in the horizontal direction (parallel to the mean current flow). We shall see that δ is a free parameter.

For such solutions, not only will $\alpha_{0,i} - \alpha_{0,j} - A_{ij} = 0$ on vertical bonds, but we must also have all $\tilde{\alpha}_{1,ij} \equiv \tilde{\alpha}_H$ on all horizontal bonds, so that the magnitude of the oscillating currents on these bonds is the same. Similarly, we expect $\tilde{\alpha}_{1,ij} \equiv \tilde{\alpha}_V$ on all vertical bonds.

This leaves the phase shifts $\tilde{\phi}_{ij}$ and the dc gauge-invariant phase differences $\alpha_{0,i} - \alpha_{0,j} - A_{ij}$ on the horizontal bonds as the only relevant parameters. Note that, if the difference on two adjacent horizontal bonds is indicated by Δ_H, then Eq. (7) implies that

$$\Delta_H(\alpha_{0,i} - \alpha_{0,j} - A_{ij}) = \Delta_H\tilde{\phi}_{ij} \ . \tag{8}$$

We now continue our process of motivating the choice

of a particular family of solutions to Eqs. (6) and (7). Since $\alpha_{0,i}-\alpha_{0,j}-A_{ij}=0$ on all vertical bonds, the constraint

$$\sum_P(\alpha_{0,i}-\alpha_{0,j}-A_{ij})=-2\pi f \tag{9}$$

implies that $\{\alpha_{0,i}-\alpha_{0,j}-A_{ij}\}$ on horizontal bonds differ by $2\pi f$ upon translation by one vertical lattice spacing.

We may recall that, in the zero-current case, array ground states have a $q\times q$ symmetry, where $f=p/q$.[7] It is natural to suppose that this symmetry is preserved in the direction perpendicular to the current in the case where current flows across the array. This suggests that perhaps the oscillating phase shifts $\tilde{\phi}_{ij}$ [from Eq. (5)] change by $2\pi f$ as well on translation by one lattice spacing in the vertical direction. In addition, we suppose that these phase shifts change by δ upon translation by one lattice spacing in the horizontal direction, as do the dc phase differences $\alpha_{0,i}-\alpha_{0,j}-A_{ij}$ on horizontal bonds. Alternatively, we can derive this from the constraint of translational plus time-translational invariance (see Fig. 1).

This state can also be described by saying that the phase differences on horizontal bonds $\langle ij\rangle$ have the form

$$\theta_{ij}=\psi_{ij}^H+f_H(\psi_{ij}^H)\ , \tag{10}$$

while those on vertical bonds have the form

$$\theta_{ij}=f_V(\psi_{ij}^V)\ , \tag{11}$$

with f_H and f_V periodic functions with period 2π. In the high-voltage limit, we are approximating f_H and f_V as harmonic functions; the more general case is treated in Sec. IV below. The phase differences $\psi_{ij}^{H,V}$ on the bonds connecting the m,n to the $m,n+1$ or $m+1,n$ sites of the lattice obey

$$\psi_{ij}^{H,V}=\psi_0^{H,V}+2\pi mf+\delta n+\omega_J t\ . \tag{12}$$

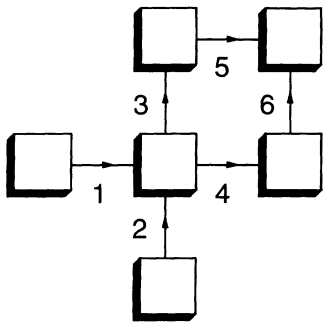

FIG. 1. In the high-voltage traveling-wave state, the phase differences have fixed phase shifts with respect to neighboring phase differences. The average current in this figure flows parallel to bonds 1, 4, and 5. Phase 4 has a nonoscillating component which is that of phase 1 increased by δ. The oscillating components of phases 4 and 6 are phase shifted by δ with respect to those of phases 1 and 3, respectively. The nonoscillating component of phase 5 is shifted by a phase $2\pi f$ with respect to that of phase 4, as are the oscillating components of these phases. The oscillating component of phase 3 is shifted by $2\pi f$ with respect to that of phase 2.

Equations (10)–(12) confirm that our solutions are essentially traveling-wave solutions.

Let us consider the oscillating part of the sum of phase differences around a plaquette. Because the phase shift of the two horizontal bonds differs by $2\pi f$, according to our assumption above, we can write these two phase shifts as $\tilde{\phi}_{ij}=\Gamma_H\pm\pi f$, where Γ_H differs from plaquette to plaquette. Similarly, since phase shifts increase by δ in moving to the right, we have that on the vertical bonds bordering this plaquette we can write $\tilde{\phi}_{ij}=\Gamma_V\pm\delta/2$. Thus, since the sum of the oscillating part of the gauge-invariant phase difference about the plaquette must be zero, we have

$$\begin{aligned}&\alpha_H[\cos(\omega_J t+\Gamma_H+\pi f)-\cos(\omega_J t+\Gamma_H-\pi f)]\\&\quad+\alpha_V[\cos(\omega_J t+\Gamma_V+\delta/2)-\cos(\omega_J t+\Gamma_V-\delta/2)]\\&\qquad=0\ ,\end{aligned} \tag{13}$$

which immediately implies

$$\Gamma_H=\Gamma_V\ , \tag{14}$$

and

$$\alpha_H\sin(\pi f)+\alpha_V\sin(\delta/2)=0\ . \tag{15}$$

Now consider four bonds coming into one node. On the two horizontal bonds, the phase shifts of the oscillating parts can be written as $\tilde{\phi}_{ij}=\bar{\Gamma}_H+\Theta\pm\delta/2$, while the oscillating phase shifts on the two vertical bonds can be written as $\tilde{\phi}_{ij}=\bar{\Gamma}_V+\Theta\pm\pi f$. Here again $\bar{\Gamma}_H$ and $\bar{\Gamma}_V$ will depend on the particular node. Equation (14) implies that these quantities at a node will obey

$$\bar{\Gamma}_H=\bar{\Gamma}_V\ . \tag{16}$$

The nonoscillating phase shifts on the horizontal bonds will be $\alpha_{0,i}-\alpha_{0,j}-A_{ij}=\bar{\Gamma}_H\pm\delta/2$, where the phase differences are defined in the same sense on the two bonds. Now such a state automatically satisfies the criterion Eq. (7), so the dc current component is conserved at the node. For the ac current to be conserved, we obtain the following criteria (note that terms of order κ are ignored inside the supercurrent term):

$$\Theta=0\ , \tag{17}$$

and

$$\alpha_H\sin(\delta/2)-\alpha_V\sin(\pi f)-\kappa\sin(\delta/2)=0\ , \tag{18}$$

where again $\kappa\equiv i_0R/v$. Combining with Eq. (15) we obtain

$$\alpha_H=\frac{\kappa}{1+[\sin^2(\pi f)/\sin^2(\delta/2)]}\ . \tag{19}$$

For this state, the total current flowing per bond is

$$i=\frac{v}{R}+i_0J_1(\alpha_H)\approx\frac{v}{R}\left[1+\kappa\frac{\alpha_H}{2}\right]\ , \tag{20}$$

where the approximation to the Bessel function is justified by the fact that the above computations ignore terms of higher order in κ.

Equation (20) can be viewed as a quadratic equation for the voltage given a fixed current i. Solving for v, we obtain

$$v=\frac{1}{2}\left[iR+\left[(iR)^2-\frac{2(i_0R)^2}{1-[\sin^2(\pi f)/\sin^2(\delta/2)]}\right]^{1/2}\right] . \tag{21}$$

The minimum and maximum voltages are obtained, respectively, for $\delta=\pi$ and 0. Thus the width of the band of allowed voltages is

$$\Delta v\equiv v(\delta=0)-v(\delta=\pi) =\frac{1}{2}\left[iR-\left[(iR)^2-\frac{2(i_0R)^2}{1+\sin^2\pi f}\right]^{1/2}\right] . \tag{22}$$

As $i\rightarrow\infty$, we obtain

$$\Delta v\approx\frac{i_0^2R}{2i}\frac{1}{1+\sin^2\pi f} , \tag{23}$$

so that the width of the band of allowed voltages goes inversely with the current i at large current.

IV. GENERALIZATION TO MODERATE VOLTAGE

Once we move away from the limit of high voltage, we must take into account higher-order effects in κ. This implies in turn that we must include the effect of phase oscillations at higher harmonics of the Josephson frequency ω_J. We proceed in analogy with the argument of Sec. III. First, we write the phase on the mn site as

$$\theta_{mn}=\alpha_{0,mn}+\sum_{k=1}^{\infty}\alpha_{k,mn}\cos(k\omega_Jt+\phi_{k,mn})+n\omega_Jt , \tag{24}$$

for a site in the mth row and nth column. On the $\langle ij\rangle$ bond, we can write

$$\alpha_{k,i}\cos(k\omega_Jt+\phi_{k,i})-\alpha_{k,j}\cos(k\omega_Jt+\phi_{k,j}) \equiv\tilde{\alpha}_{k,ij}\cos(k\omega_Jt+\tilde{\phi}_{k,ij}) . \tag{25}$$

As in Sec. III above, we restrict ourselves to states with a combined translational and time-translational symmetry. This implies that all $\tilde{\alpha}_{k,ij}$ are the same on horizontal (or vertical) bonds, defining $\tilde{\alpha}_{k,H}$ and $\tilde{\alpha}_{k,V}$, respectively. Again, we expect that the quantity $\alpha_{0,i}-\alpha_{0,j}-A_{ij}=0$ on vertical bonds, and its value on horizontal bonds increments by $2\pi f$ if one moves one lattice spacing in the vertical direction. The phase shifts $\tilde{\phi}_{k,ij}$, by contrast, must increment by $2\pi kf$ upon translation by one lattice spacing in the vertical direction, in order that the combined translational and time-translational symmetry of the high-voltage state be maintained. We also expect that translation by one lattice spacing in the horizontal direction adds $k\delta$ to the phase differences $\tilde{\phi}_{k,ij}$, and adds δ to $\alpha_{0,i}-\alpha_{0,j}-A_{ij}$.

The sum of the oscillating phase differences about a plaquette must equal zero. Suppose that the phase shifts $\tilde{\phi}_{k,ij}=\Gamma_{k,H}\pm\pi kf$ on the horizontal bonds bounding a plaquette, and $\tilde{\phi}_{k,ij}=\Gamma_{k,V}\pm k\delta/2$ on the vertical bonds bounding a plaquette. Then following the same reasoning that led to Eqs. (14) and (15), we obtain

$$\Gamma_{k,H}=\Gamma_{k,V} , \tag{26}$$

and

$$\alpha_{k,H}\sin(k\pi f)+\alpha_{k,V}\sin(k\delta/2)=0 . \tag{27}$$

The reader will note that Eq. (27) yields selection rules on the harmonics of ω_J that appear for rational values of f or δ/π. For example, if $f=\frac{1}{2}$, all of the even harmonics of ω_J are missing from the oscillating phase differences on the vertical bonds (unless $\delta=\pi$). The observation of the validity of these selection rules in numerical simulations is a sensitive test of the appearance of these special states (see Sec. V below).

The imposition of the constraint that the ac currents be conserved at every site is quite tedious in general. We will outline the procedure. Let us suppose that the dc phase differences on the two horizontal bonds attached to a site are $\alpha_{0,i}-\alpha_{0,j}-A_{ij}=\bar{\Gamma}_H\pm\delta/2$. The oscillating phase shifts on the horizontal bonds are $\tilde{\phi}_{k,ij}=\bar{\Gamma}_H+\Theta_k\pm k\delta/2$, and the oscillating phase shifts on the vertical bonds are $\tilde{\phi}_{k,ij}=\bar{\Gamma}_V+\Theta_k\pm k\pi f$. From Eq. (26) we see that $\bar{\Gamma}_H=\bar{\Gamma}_V$. The supercurrent term can be expanded in harmonics of the frequency ω_J:

$$i_0\sin\left[\omega_Jt+\delta/2+\sum_{k=1}^{\infty}\alpha_{k,H}\cos(k\omega_Jt+\Theta_k+k\delta/2)\right] =i_0\left[a_0+\sum_{l=1}^{\infty}a_l\sin(l\omega_Jt+\psi_l+l\delta/2)\right] , \tag{28}$$

where we have absorbed $\bar{\Gamma}_H$ into the origin of t as well as into the phase shifts $\{\Theta_k\}$. The coefficients $\{a_l\}$ and the phase shifts ψ_l are complicated (but, in principle, calculable) functions of $\{\alpha_{k,H}\}$ and $\{\Theta_k\}$, but they are not functions of δ.

Since a_0 is independent of δ, provided that all other constants are held fixed, the dc supercurrent into a site is the same as that out of a site. Conservation of the oscillating currents into a site leads to the criterion

$$[\alpha_{k,H}\sin(k\delta/2)-\alpha_{k,V}\sin(k\pi f)]\cos(k\omega_Jt+\Theta_k) -\frac{\kappa}{k}a_k\sin(k\delta/2)\cos(k\omega_Jt+\psi_k)=0 . \tag{29}$$

In practice, Eq. (29) may be solved order by order in κ. Thus, for instance, we know that to lowest order in κ, $\Theta_1=0$ [see Eq. (17) above]. This allows the lowest-order term [of $O(\kappa)$] in ψ_2 to be computed from Eq. (28). This in turn allows the computation of the lowest order in Θ_2 and $\alpha_{2,H}$ or $\alpha_{2,V}$ to be computed from Eqs. (27) and (29). This procedure can be continued until the patience of the researcher, or that of his symbolic manipulation program, is exhausted.

V. NUMERICAL RESULTS

This system can also be numerically integrated. The method is standard—the condition of current conservation at the site i is first written as a matrix equation

$$M_{ij}\frac{d\theta_j}{dt}=F(\{\theta_{i'}-\theta_i\}) , \tag{30}$$

where i' denotes a neighbor to site i. The matrix $\mathbf{M}$ is then inverted, yielding a set of coupled first-order differential equations, which can be integrated by means of, e.g., the fourth-order Runge-Kutta method.[8] We normally fixed the currents at the left- and right-hand sides of an $N\times N$ array, and studied the consequent phase dynamics far from the boundaries of the array. In the direction transverse to current flow, we used periodic boundary conditions. We also normally used lattices of size 60×60, although some runs were performed with lattices of size 30×30. Most of our simulations were performed with initial conditions corresponding to zero-voltage ground states. Typically, these states reproducibly relaxed to traveling-wave states. At any current, we only ever observed a single value of δ to be stable for long times.

Figure 2 shows the typical behavior of the gauge-invariant phase differences for $f=\frac{1}{3}$. The phases for neighboring bonds differ by $2\pi/3$ for bonds separated by one vertical lattice spacing, and by a fixed value δ for bonds separated by one horizontal lattice spacing. This behavior is observed throughout the array, except immediately in the vicinity of the boundaries. This confirms our ansatz for the form of the solution. This behavior has also been observed over a wide range of currents for the values of the frustration $f=\frac{1}{2}$, $\frac{1}{3}$, and $\frac{2}{5}$.

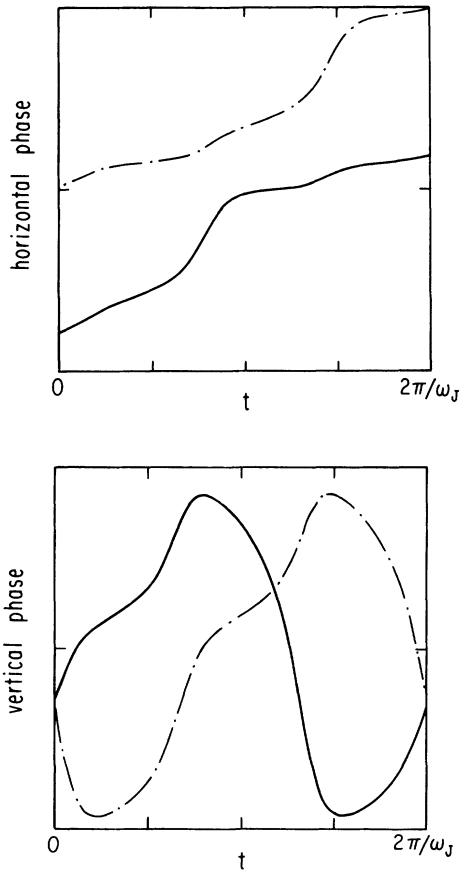

FIG. 2. (a) Gauge-invariant phase differences of two neighboring horizontal bonds along the horizontal direction; the phase shift of δ is constant. (b) Gauge-invariant phase differences of two neighboring vertical bonds along the horizontal direction; the phase shift between these two phase differences is also δ.

These states can be visualized by their vortex configurations. The sum around a plaquette of the instantaneous gauge-invariant phase differences obeys

$$\sum_P(\theta_i-\theta_j-A_{ij})=2\pi(n_v-f) , \tag{31}$$

with n_v an integer, where the phase differences are restricted to lie between $\pm\pi$ (if we do not impose this restriction, $n_v=0$). We term n_v the vorticity of the plaquette. The sign of δ determines the orientation of the vortex configuration. In the traveling-wave state, the vorticities of the plaquettes are out of phase by δ along the horizontal direction and are out of phase by $2\pi f$ along the vertical direction. In a particular plaquette, the vorticity is 1 during a fraction f of the period $2\pi/\omega_J$ and zero during the rest of it. Thus each vortex moves vertically q times per period. The vortex configuration is periodic with period q along the vertical direction; the configuration along the horizontal direction is determined by δ.

Figure 3 shows the vortex configurations obtained for various values of δ for $f=\frac{1}{3}$. $\delta=\pm 2\pi/3$ yields the vortex configuration of the "staircase state," in which stripes of vortices run along the diagonals of the lattice.[7] This is known to be the form of the zero-voltage ground state for this value of f. For general f, the staircase-state vorticity can be obtained by choosing $\delta=\pm 2\pi f$.

The value of δ may be obtained by inspection of the vortex configuration. For $f=\frac{1}{3}$ and $\pi/6<\delta<5\pi/6$, the configuration looks locally staircaselike, with "domain walls" of two possible types, according to whether δ is greater or less than $2\pi/3$. However, these are not actually domain walls, since the nature of the solution at these "walls" does not differ from that in the rest of the array. If the average distance between these "walls" is L, δ is given by

$$\delta=\frac{2\pi}{3}\left[1+\frac{1}{L}\right] . \tag{32}$$

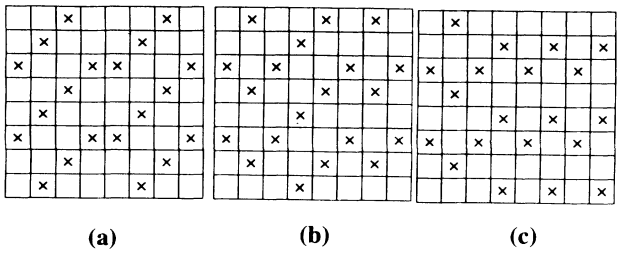

FIG. 3. (a) Vortex configuration for $f=\frac{1}{3}$; the value of $\delta=\pi/2$. A "heavy" domain wall can be seen in the staircase vortex configuration. (b) In this case, $\delta=0.7\pi$; a "light" domain wall can be seen in the staircase vortex configuration. (c) In this case, $\delta=0.95\pi$. If $\delta=\pi$ exactly, the vortices form undefected horizontal zigzag lines.

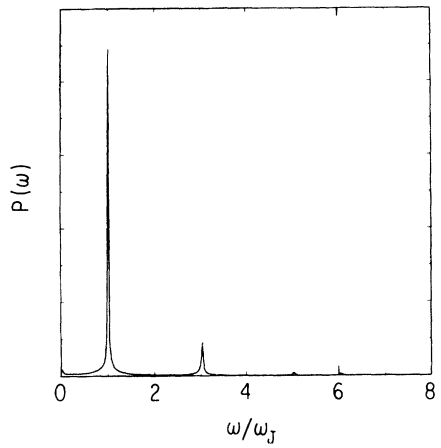

FIG. 4. Power spectrum $P(\omega)$ of horizontal phase variations for $f=\frac{1}{3}$ and $\delta\approx\pi$. The second and fourth harmonics of the Josephson frequency are absent, in accord with the selection rule from Eq. (27). Note that the sixth harmonic, which does appear, is not excluded by this equation.

Here the sign of L indexes the type of domain wall observed (see Fig. 3). A simple analysis shows that these two types of "domain walls" move in opposite directions. The apparent speed is

$$u=\frac{2\pi L}{\omega_J} . \tag{33}$$

The values of δ obtained by inspection are in excellent agreement with those obtained from the time series. In terms of δ we can describe the observations in Ref. 4 by saying that for low currents δ increases from a value a little less than π to π at a current per junction of $i\simeq 0.7 i_0$. Above this current δ jumps to a value a little greater than $2\pi/3$ and then decreases as the current is increased.

An additional check on the appearance of the traveling-wave state is to investigate the satisfaction of the selection rules for harmonics of ω_J; we alluded to these rules after Eq. (27) above. This may be done by taking the power spectrum of the phase oscillations on particular horizontal or vertical bonds; the results are in agreement with the predictions from Eq. (27) (see Fig. 4). We also found that Eq. (21) for the I-V relation as a function of δ held to high accuracy in these simulations.

One of the striking features of these simulations was the appearance of fronts, commencing at the boundaries, separating regions with differing values of δ and differing voltages (see Fig. 5). The fronts were parallel to the boundaries at which current was injected, and were thus perpendicular to the direction of mean current flow. These fronts always moved in the direction of decreasing voltage, or Josephson frequency. Thus, as the front moved by a particular bond, the average voltage on that bond increased. Since the fronts moved at fixed speeds, the overall voltage across the array tended to increase linearly, and saturate at a higher value once the front had passed across the entire system. The passage of these fronts constitutes a means by which the system selects a particular value of δ, and we expect that a quantitative understanding of the front structure will assist in solving the problem of which value of δ is chosen by the system at a particular current.

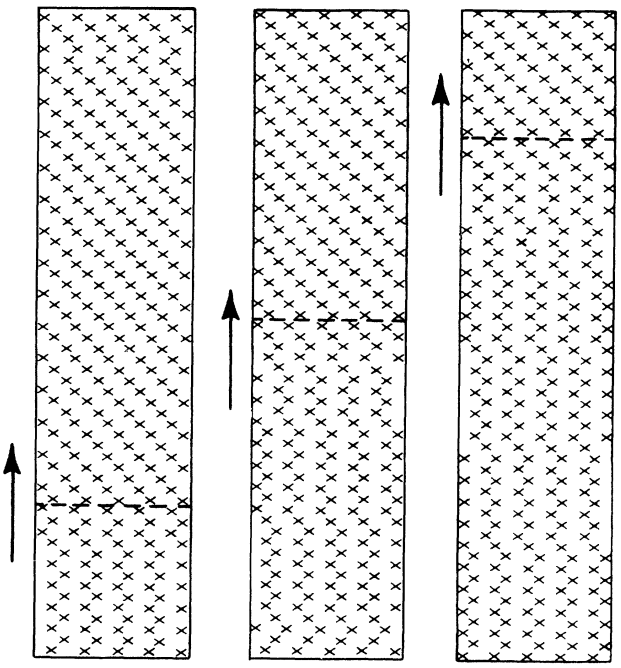

FIG. 5. Vortex configurations for $f=\frac{1}{3}$ corresponding to a front propagating from the left to the right. On the left-hand side of the front, $\delta\approx\pi$, while on the right-hand side of the front, $\delta=2\pi/3$.

We also studied the role played by the symmetry of the initial configuration in determining the boundary at which the front develops. Reversing the sign of the magnetic field is equivalent to choosing the initial configuration tilted along the other diagonal, with the current flowing in the same direction. This reversed the boundary at which the front developed.

On the other hand, when we started with an initial configuration with no preferred diagonal axis (i.e., with $\delta=0$ or π), fronts developed at both boundaries. The final configuration corresponded to a fixed front separating two regions of opposite δ and the same voltage. We observed relaxation through front propagation for $f=\frac{1}{2},\frac{1}{3}$, and $\frac{2}{5}$ at sufficiently low currents.

ACKNOWLEDGMENTS

I.M. wishes to acknowledge helpful conversations with Eric Kramer. This research was supported by the Materials Research Laboratory at the University of Chicago.

[1]An excellent general review is the conference volume *Coherence in Superconducting Networks, Proceedings of the NATO Advanced Research Workshop, Delft, The Netherlands, 1987,* [Physica B **152** (1988)].

[2]T. D. Clark, Phys. Rev. B **8**, 137 (1973); C. Leeman, P. Lerch, and P. Martinoli, Physica (Amsterdam) **126B**, 475 (1984); S. P. Benz, M. S. Rzchowski, M. Tinkham, and C. J. Lobb, Phys. Rev. Lett. **64**, 693 (1990).

[3]K. H. Lee, D. Stroud, and J. S. Chung, Phys. Rev. Lett. **64**, 962 (1990); K. H. Lee and D. Stroud, Phys. Rev. B **43**, 5280 (1991); M. S. Rzchowski, L. L. Sohn, and M. Tinkham, *ibid.* **43**, 8682 (1991); T. C. Halsey, *ibid.* **41**, 11 634 (1990); S. J. Lee and T. C. Halsey, *ibid.* **47**, 5133 (1993).

[4]This problem has also been studied by F. Falo, A. R. Bishop, and P. S. Lomdahl, Phys. Rev. B **41**, 10 983 (1990); see also A. R. Bishop, in *Nonlinear Structures in Physical Systems,* edited by L. Lam and H. C. Morris (Springer-Verlag, New York, 1990).

[5]For the general physics of Josephson junctions, see M. Tinkham, *Introduction to Superconductivity* (McGraw-Hill, New York, 1975), Chap. 6.

[6]B. D. Josephson, Phys. Lett. **1**, 251 (1962).

[7]S. Teitel and C. Jayaprakash, Phys. Rev. Lett. **51**, 1999 (1983); T. C. Halsey, Phys. Rev. B **31**, 5728 (1985).

[8]A discussion of the method is found in J. S. Chung, K. H. Lee, and D. Stroud, Phys. Rev. B **40**, 6570 (1989); for Runge-Kutta integration, see W. H. Press, B. P. Flannery, S. A. Teukolsky, and W. T. Vetterling, *Numerical Recipes: The Art of Scientific Computing* (Cambridge University, Cambridge, England, 1986), Chap. 15.